GEOPHYSICAL RESEARCH LETTERS, VOL. 23, NO. 2, PAGES 133-136, JANUARY 15, 1996

Space-time structure of optical flashes and ionization changes produced by lighting-EMP

Umran S. Inan, Wesley A. Sampson
STAR Laboratory, Stanford University, Stanford, California

Yuri N. Taranenko
Los Alamos National Laboratory, Los Alamos, New Mexico

Abstract. Intense electromagnetic pulses (EMPs) released by lightning discharges produce bright optical emissions at 80-95 km altitudes emitted in a thin (~30 km) cylindrical shell expanding to radial distances of up to >150 km, lasting for ~400μs, and appearing in limb-view as a thin layer with ~400 km lateral extent.

Introduction

Energy release triggered by lightning discharges is believed to lead to optical emissions and significant ionization changes resulting from the acceleration of ambient electrons by intense EMPs [*Inan et al.*, 1991; *Taranenko et al.*, 1993a,b; *Rowland et al.*, 1995], or by quasi-electrostatic (QE) fields following lightning discharges [*Pasko et al.*, 1995a]. The lightning EMP has a duration <1 ms [*Uman*, 1987, p. 110], typically ~50 to 100μs, and produces heating of electrons and optical emissions which last as long as the driving fields, primarily at 80-95 km altitudes [*Taranenko et al.*, 1993a]. The QE field exists during the time (a few tens of ms at low altitudes to a few ms at 70 km) that the partially conducting atmosphere responds to the 'rearrangement' of thundercloud charge (by the discharge) and produces the largest heating at 60-85 km altitudes [*Pasko et al.*, 1995a].

Energetic positive cloud-to-ground (CG) discharges lead to luminous glows (sprites) extending in altitude from ~50 to 90 km [*Sentman et al.*, 1995; *Boccippio et al.*, 1995] with lateral dimensions of 10-50 km, and lasting for ~10 to 50 ms. The bulk of the luminosity of sprites is more consistent with heating by QE fields than by EMP. In recent photometric measurements [*Fukunishi et al.*, 1995] sprites are often preceded by short (~ 300 μs) and diffuse brightening (called 'elves') at altitudes ~90 km with lateral extent of ~ 300 km, characteristics expected to be produced by the EMP-ionosphere interaction.

The physics of the lightning EMP-ionosphere interaction can be summarized as follows: The peak spectral content of EMPs radiated by lightning is typically in the VLF range (3-30 kHz). Reflection of VLF waves in a nighttime ionosphere occurs at the altitude where the normalized electron collision and plasma frequencies are equal (~85 km for typical nighttime ionosphere) [*Ratcliffe*, 1959, p. 90]. The maximum absorption of wave energy (i.e., heating of the electrons) also occurs near the same altitude [*Inan*, 1990], and moves to higher altitudes in cases of intense heating [*Taranenko et al.*, 1993a]. Excitation of optical emissions is a process with an energetic threshold leading to nonlinear dependence of emission intensities on the EMP intensity. The 1st positive band of N_2 is excited by impact on N_2 of electrons with energies >7 eV whereas the ambient electrons in the upper atmosphere are initially at ~0.03 eV. Since the maximum heating occurs at 85-95 km, the optical emissions are excited in this altitude range.

Previous modeling of the lightning EMP-ionosphere interaction started by assuming a Maxwellian electron energy distribution [*Inan et al.* 1991; *Rodriguez et al.*, 1992], followed by a 1-D fully kinetic model [*Taranenko et al.*, 1993a,b], and a 2-D model of ionization based the EMP heating the ambient plasma to saturation (6 eV) [*Rowland et al.*, 1995]. In our model, we use electron mobility, ionization, and two-body attachment rates based on experimental data and quantify the temporal and spatial variations of optical emissions produced under different conditions.

Model Formulation

The CG lightning 'radiator' is taken to be a vertically oriented small ($\ll$2 km) dipole antenna on conducting ground, with a current of $I_z(t)=I_p\text{sech}[10^{-5}(t-t_o)]$ to approximate a lightning first return-stroke current (Figure 1a), consistent with typical lengths of return strokes at the time of peak radiation of no more than a few hundred meters [*Krider and Guo*, 1983]. The vector potential and the field components of the EMP in free space are analytically determined from $I_z(t)$. The $E_z(t)$ at z=0 and r=100 km is shown in Figure 1b. Extensive past work has been done on modeling of lightning return-stroke currents [*Thottappillil and Uman*, 1993] and EMP waveforms exhibit a wide range of complexity [e.g., *Uman*, 1987; p.110-117; *Lanzerotti et al.*, 1989]. Our simple model is sufficient to represent the basic physics of the EMP-ionosphere interaction and to determine the ionospheric responses.

The EMP intensity is parametrized by the maximum total electric field E_{100} at z=0 and r=100 km (Figure

Paper number 95GL03816
0094-8534/96/95GL-03816$03.00

1). Empirically, E_{100}=50 V/m corresponds to a peak current of $I_p \simeq$170 kA [*Orville*,1991]. Although E_{100}>25 V/m may be rare for negative CG flashes, positive CG flashes are generally more intense, and can involve $I_p \simeq$200-300 kA [*Uman*, 1987; p.188], and a few percent $I_p \geq$300 kA [*Berger et al.*, 1975]. Examples of positive CG lightning with E_{100}>50 V/m have been reported [*Brook et al.*, 1989] and some positive CG flashes associated with ionospheric disturbances involved I_p>200 kA or E_{100}>50 V/m [*Inan et al.*, 1993].

The free space fields are used up to 70 km altitude, above which we use a mesh with grid spacings of Δz=125 m and Δr=500 m and a two-step Lax-Wendroff scheme for the solution of Maxwell's Equations. The conduction current, ionization, and attachment rates are determined by the electric field and are used to dynamically alter the fields and particle densities. We neglect the earth's magnetic field, since the effective collision frequency of the heated electrons is much larger than the electron gyrofrequency. The conductivity as a function of the electric field is based on an analytical fit to experimental data [*Davies*, 1983]. The ionization rate is based on analytical fits to atmospheric and ionospheric breakdown rates given by *Papadopoulos et al.* [1993] and based on computer simulations and experimental data. Analytical fits to experimental data [*Davies*, 1983] are also used for the effective reaction rates (as a function of electric field) of the two-body, dissociative attachment of electrons to O_2 molecules. All of the analytical fits used are in good agreement with previous kinetic calculations [*Taranenko et al.* 1993a].

We consider the first positive band of N_2 with excitation rates obtained from kinetic calculations [*Taranenko et al.*, 1993b]. The temporal and spatial structure of emissions at other wavelengths should be similar. Altitude profiles of the electron density N_e and density of neutrals N were taken to be as shown in Figure 1c.

Space-time Dynamics of Optical Flashes

Figure 2a shows snapshots of the altitude and radial distributions of the total electric field, volume emission intensity (Φ_v) of the first positive band of N_2, and the ionization change ($\Delta N_e/N_e$) for E_{100}=50 V/m, with t=0 being the start of the current pulse (Figure 1a).

At t=375μs the wavefront has reached ~85-95 km altitudes and the reflection process has started [*Ratcliffe*, 1959, p.90]. The front and tail ends of the 100-μs long EMP (separated by 30-km) are visible. The front of the reflected pulse is at ~87 km altitude, with much reduced intensity. The electric field pattern consists of an expanding cylindrical shell of 30-km (100μs at the speed of light) thickness.

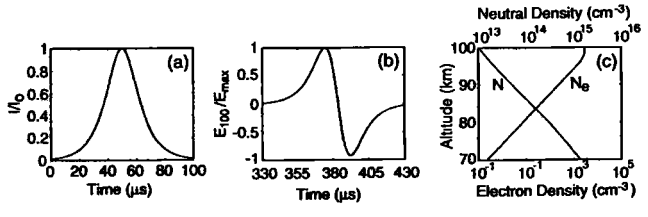

Figure 1. (a) Assumed dipole radiator current waveform; (b) Vertical electric field as measured at r=100 km on the ground ($E_{100}(t)$); (c) Ambient profiles of electron (N_e) and neutral (N) densities.

The double peaks in Φ_v correspond to the positive and negative peaks of the electric field (Figure 1b). The emission region is a cylindrical shell of thickness ~30 km with a ~10 km vertical extent, which radially expands (Figure 3a) at a rate initially faster than the speed of light but decreasing as $(\sqrt{t})^{-1}$. This effect is analogous to the motion of water waves along the shoreline when they arrive on a beach at an angle. Since the EMP intensity decreases with r, so does Φ_v. At t=675μs, when the outer edge of the emission shell at z=90 km has reached r=180 km, Φ_v has decreased to 2.67×10^7 ph/cm^3-s; the EMP electric field, varying as r^{-1}, decreases below the threshold of excitation of the N_2 first positive band at $r \simeq$250 km.

Figure 2c shows the space-time structure of the optical flash as observed from point P_1 in Figure 2b. Frames are shown at 65μs intervals and represent the light accumulated over 4μs. At t=1165μs the photons emitted from the Front (F in Figure 2b) of the emission shell begin to reach P_1. For example, the light emitted at t=375μs from the outer edge of the shell ($r \simeq$40 km) arrives at P_1 at t=1241μs, whereas that which is emitted *later* at t=675μs when the outer edge is at $r \simeq$180 km arrives *earlier*, at t=1075μs. The dynamics of the emitting shell leads to 'focusing' (in time) of light from the Front, producing the highest intensities (dark color) observed at the center of the first two frames. By the third frame (t=1300μs), the contribution from the Sides (S) begins to arrive, and at t=1365μs, the Front has ceased to emit as viewed at P_1; the light originating at t=375μs from the inner edge of the shell (i.e., $r \simeq$15 km at 90-km altitude) arrives at P_1 at t=1325μs. The other frames in Figure 2c can be similarly interpreted; at t=1500μs the light from the Back (B) of the emitting shell begins to arrive, since the first light emitted at t=375μs from the inner edge of the Back (at r=15 km) arrives at t=1425μs. The 'defocusing' in time of light from the Back leads to lower intensities (dark blue). The time-average of the snapshots appears as a narrow layer with ~400 km lateral extent (lowest panel of Figure 2c), consistent with a CG lightning-associated 'airglow' enhancement observed in limb-view [*Boeck et al.*, 1992].

As viewed from an upward looking (e.g., from an aircraft immediately above the thundercloud) we see a ring-shaped structure of thickness ~30 km, with a rapidly expanding radius (Figure 2d, left panel). The right hand panel of Figure 2d shows the intensity averaged over a 16-ms video frame, predicting the maximum to lie between $r \simeq$40 to $r \simeq$110 km.

Figure 3a,b show the temporal profile of the optical flash as measured by broad-beam photometers located at P_1 and P_2, computed by accounting for both the travel time of the light and its r^{-2} divergence. At P_1, the peak intensity is observed at ~1.2 ms (t = 0 being the start of the current pulse). The highly nonlinear dependence of the peak emission intensity on E_{100} is apparent from Figure 3a, ranging from $\sim 10^{11}$ ph/cm^2-s for E_{100}=25 V/m to $\sim 4.5 \times 10^{12}$ ph/cm^2-s for E_{100}=100 V/m. The response curve at point P_2 has a somewhat delayed onset; the sharply peaked earlier part of this response is consistent with recent observations [*Fukunishi et al.*, 1995], of optical emissions of ~300-400μs duration. Figure 3c shows the response curves as would be observed with two different photometers having a finite (1° × 9°) field-of-view and aimed at different elevation

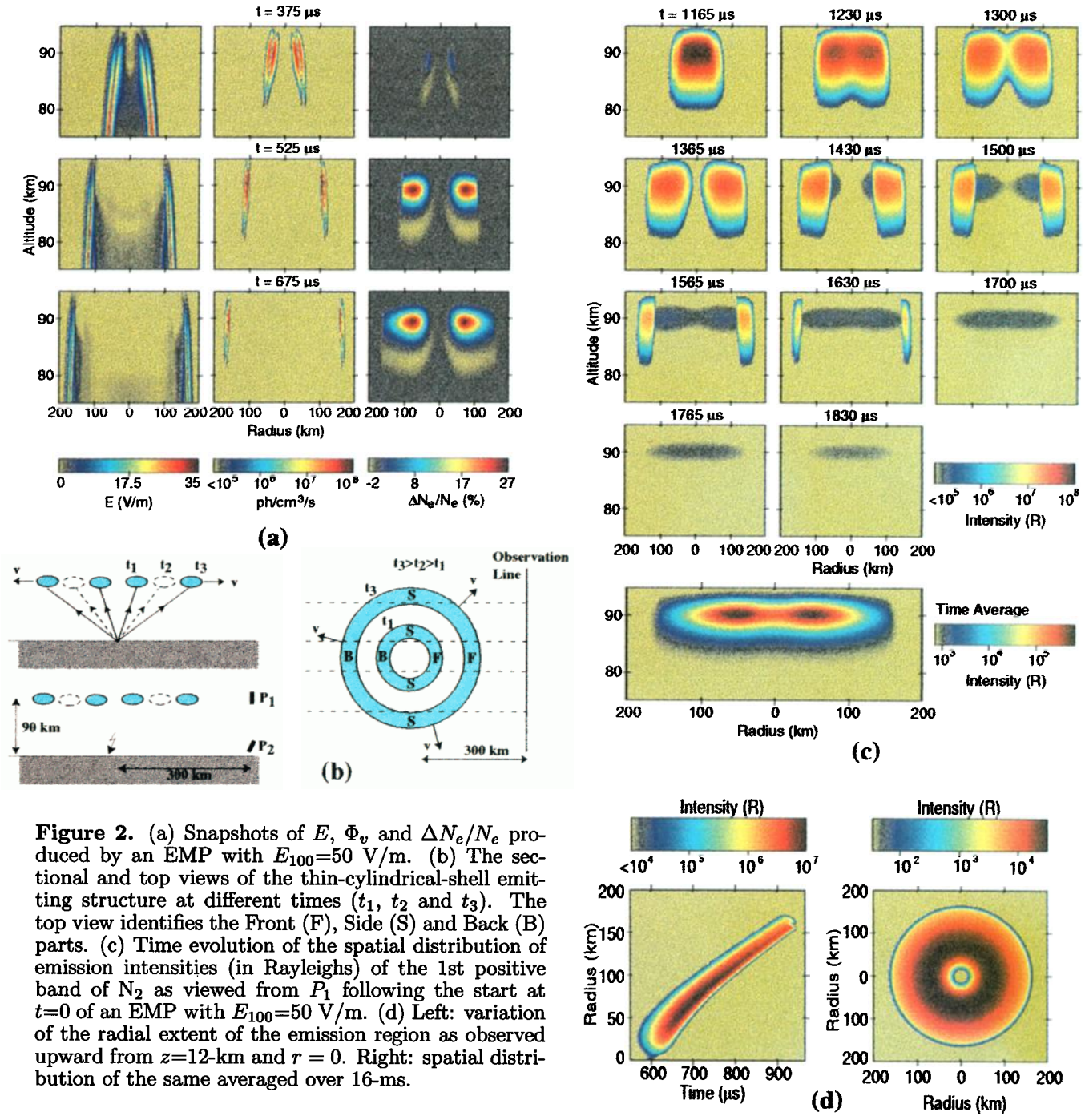

Figure 2. (a) Snapshots of E, Φ_v and $\Delta N_e/N_e$ produced by an EMP with E_{100}=50 V/m. (b) The sectional and top views of the thin-cylindrical-shell emitting structure at different times (t_1, t_2 and t_3). The top view identifies the Front (F), Side (S) and Back (B) parts. (c) Time evolution of the spatial distribution of emission intensities (in Rayleighs) of the 1st positive band of N_2 as viewed from P_1 following the start at t=0 of an EMP with E_{100}=50 V/m. (d) Left: variation of the radial extent of the emission region as observed upward from z=12-km and $r = 0$. Right: spatial distribution of the same averaged over 16-ms.

angles (Figure 3d). The 19.4° photometer sees the light from the Front of the ring arriving earlier and at higher intensity. The difference in time of the peaks of the two responses gives the appearance of vertical motion along the dashed line (at a speed of $\sim 4 \times 10^4$ km/s), although it is simply manifested by the lateral motion of the expanding emission ring.

Ionization Changes

The ionization changes accumulate in time, since the relaxation time is much longer than 100μs. From Figure 2a, at t=675μs, the electric field intensity at large r has reduced to below threshold levels. Dissociative attachment (occuring for ~6 eV electrons) dominates at lower altitudes (mild heating) causing density decreases. At higher altitudes, electrons are heated beyond ~6 eV and impact ionization (threshold for N_2 is 15.6 eV) dominates, leading to density increases. The transverse extent of the ionization region is ~±150 km, with a minimum at the center, due to the assumed vertical geometry of the source current. The region of enhanced ionization is enveloped by a 'halo' of reduced ionization (due to attachment), extending down to ~80 km altitude. Although the magnitude of the density reduction is relatively small (~3%), it may contribute to the observed 'early' VLF disturbances [*Inan et al.*, 1993], since ionization above the nighttime VLF reflection height (~85 km) is less likely to affect a VLF signal.

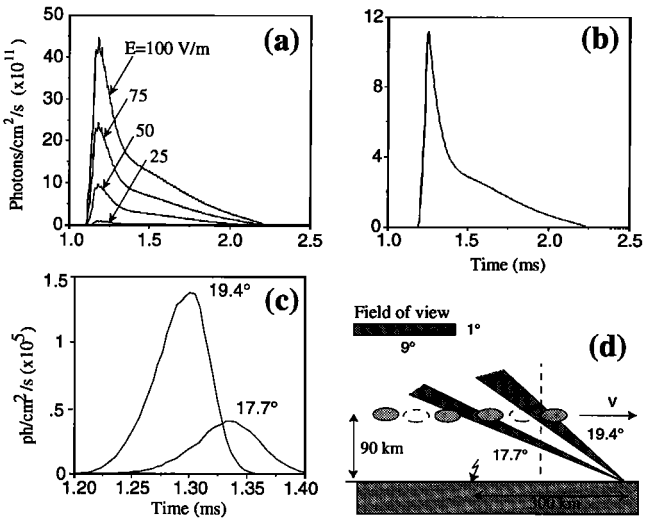

Figure 3. Temporal signatures of the optical flashes observed with (a,b) broad-beam photometers at P_1 for E_{100}=25,50,75, and 100 V/m and at P_2 for E_{100}=50 V/m, (c) two $1° \times 9°$ photometers at different elevations as shown in (d).

Summary

Intense electromagnetic pulses produced by CG lightning return-strokes with peak currents I_p>80 kA (or E_{100}>25 V/m) produce bright (>10^7 R for E_{100}=50 V/m) optical flashes and significant ionization changes at 80-95 km altitudes. The first positive band of N_2 emits in a thin (~30 km) cylindrical shell expanding in time at speeds greater than c to radial distances of up to ~250 km (for E_{100}=50 V/m). The duration of the optical flashes is estimated to be 300-500μs, depending on the observation location. In limb-view, and averaged over times >1 ms, the optical emission appears as a thin layer of lateral extent ~300-400 km. The EMP-induced ionization changes are produced in a doughnut-shaped region lying between radial distances of ~25 to ~150 km, and consisting of ionization of a few to hundreds of percent at 85-95 km and depletions of a few percent at 80-85 km altitudes.

Acknowledgments. This research was supported under grant NSF-ATM-9412287. We thank V. Pasko and T. Bell for useful discussions. Y. Taranenko was supported by a LANL post-doctoral fellowship.

References

Berger, K., R. B. Anderson, and H. Kroninger, Parameters of lightning flashes, *Electra, 80*, 23, 1975.

Boeck, W. L., O. H. Vaughan, Jr., R. Blakeslee, B. Vonnegut, and M. Brook, Lightning induced brightening in the airglow layer, *Geophys. Res. Lett.*, 19, 99, 1992.

Boccippio, D. J., E. R. Williams, S. J. Heckman, W. A. Lyons, I. Baker, and R. Boldi, Sprites, ELF transients and positive ground strokes, *Science, 269*, 1088, 1995.

Brook, M., R. W. Henderson, and R. B. Pyle, Positive lightning strokes to ground, *J. Geophys. Res., 94*, 13295, 1989.

Davies, D.K., Measurements of swarm parameters in dry air, *Theoretical Notes*, Note 346, Westinghouse R&D Center, Pittsburg, May, 1983.

Fukunishi, H., Y. Takahashi, M. Kubota, K. Sakanoi, U. S. Inan, W. A. Lyons, Elves: Lightning-induced transient luminous events in the lower ionosphere, submitted to *Geophy. Res. Lett.* , 1995.

Inan, U. S., VLF heating of the lower ionosphere, *Geophys. Res. Lett., 17*, 729, 1990.

Inan, U. S., T. F. Bell, J. V. Rodriguez, Heating and ionization of the lower ionosphere by lightning, *Geophys. Res. Lett., 18*, 705, 1991.

Inan, U. S., J. V. Rodriguez, and V. P. Idone, VLF signatures of lightning-induced heating and ionization of the nighttime D-region, *Geophys. Res. Lett., 20*, 2355, 1993.

Krider, E. P., and C. Guo, The peak electromagnetic power radiated by lightning return strokes, *J. Geophys. Res., 88*, 8471, 1983.

Lanzerotti, L. J., D. J. Thomson, C. G. MacLennan, K. Rinnert, E. P. Krider, M. A. Uman, Power spectra at radio frequency of lightning return stroke waveforms, *J. Geophys. Res., 94*, 13221, 1989.

Orville, R. E., Calibration of a magnetic direction finding network using measured triggered lightning return stroke peak currents, *J. Geophys. Res., 96*, 17135, 1991.

Papadopoulos, K., G. Milikh, A. Gurevich, A. Drobot, and R. Shanny, Ionization rates for atmospheric and ionospheric breakdown, *J. Geophys. Res., 98*, 17593, 1993.

Pasko, V. P., U. S. Inan, Y. N. Taranenko, and T. F. Bell, Heating, ionization and upward discharges in the mesosphere due to intense quasi-electrostatic thundercloud fields, *Geophys. Res. Lett., 22*, 365, 1995.

Ratcliffe, J. A., The magneto-ionic theory and its applications to the ionosphere, Cambridge University Press, Cambridge, 1959.

Rodriguez, J. V., U. S. Inan, T. F. Bell, D region disturbances caused by electromagnetic pulses from lightning, *Geophys. Res. Lett., 19*, 2067, 1992.

Rowland, H. L., R. F. Fernsler, J. D. Huba, and P. A. Bernhardt, Lightning Driven EMP in the Upper Atmosphere, *Geophys. Res. lett., 22*, 361, 1995.

Sentman, D. D., E. M. Wescott, D. L. Osborne, D. L. Hampton, M. J. Heavner, Preliminary results from the Sprites94 aircraft campaign: Red Sprites, *Geophys. Res. Lett., 22*, 1205, 1995.

Taranenko, Y. N., U. S. Inan, and T. F. Bell, The interaction with the lower ionosphere of electromagnetic pulses from lightning: heating, attachment, and ionization, *Geophys. Res. Lett., 20*, 1539, 1993a.

Taranenko, Y. N., U. S. Inan, and T. F. Bell, The interaction with the lower ionosphere of electromagnetic pulses from lightning: excitation of optical emissions, *Geophys. Res. Lett., 20*, 2675, 1993b.

Thottappillil, R., and M. A. Uman, Comparison of lightning return-stroke models, *J. Geophys. Res., 98*, 22903, 1993b.

Uman, M.A., *The lightning discharge*, Academic Press, Orlando, 1987.

U. S. Inan, W. A. Sampson, STAR Laboratory, Stanford University, Stanford, CA 94305.

Y. N. Taranenko, NIS-1, MS-D466, Los Alamos National Laboratory, Los Alamos, NM 87545

(received September 21, 1995;
revised November 22, 1995;
accepted December 18, 1995.)